Pergamon

Computers & Structures Vol. 64, No. 1–4, pp. 759–770, 1997

Printed in Great Britain
0045-7949/97 $17.00 + 0.00

PII: S0045-7949(96)00171-X

STRUCTURAL SAFETY ANALYSIS WITH ENGINEERING INTEGRITY ASSESSMENT TOOLS

H. Talja†, H. Raiko‡, T. P. J. Mikkola§ and Z. L. Zhang¶

†VTT Manufacturing Technology, P.O. Box 1704, FIN-02044 VTT, Finland
‡VTT Energy, P.O. Box 1604, FIN-02044 VTT, Finland
§VTT Manufacturing Technology, P.O. Box 1705, FIN-02044 VTT, Finland
¶SINTEF Materials Technology, N-7034 Trondheim, Norway

Abstract—This paper presents computer tools developed at the Technical Research Centre of Finland (VTT) for the assessment of flawed structures. They include flexible tools for assessing complicated structure-loading-crack configurations with the finite element method—most often used for failure analysis—and effective tools for rapid structural integrity assessments, even during the structural design phase. An integrated PC-based program system for engineering fracture analyses is described. The programs are applied to three practical examples and the feasibility of the system is shown by comparing the results with finite element (FE) results. © 1997 Civil-Comp Ltd and Elsevier Science Ltd.

1. INTRODUCTION

Sharp cracks are the most dangerous structural defects due to the extreme stresses at the crack tip. In order to solve a practical integrity problem for a cracked structure, answers must be found to the following questions:

(1) What kind of failure mechanism is expected in each specific case?
(2) How wide is the safety margin for a structure containing detected or postulated cracks of given size?
(3) What is the allowable crack size?
(4) How often should the structure be inspected by nondestructive examination (NDE) to ensure that no failure occurs between successive inspections?
(5) What is the required detection limit of the NDE method to avoid unexpected failures?

Besides effective and well-tested analysis methods and tools, information is needed about the structural geometry and dimensions, location and size of cracks, type and strength of loading, material data including mechanical and physical properties and fracture parameter values (Fig. 1). Safety assessment for structures like reactor pressure vessels in nuclear power plants include conservative calculations. For this purpose, postulated cracks are defined in the most dangerous locations and orientations, taking into account, e.g. the manufacturing history—welding in particular may produce small initial defects.

Depending on the type and manufacturing history of the material, loading rate, crack size, and environmental parameters such as temperature, chemical effects and irradiation, etc., different failure types can occur in the same structural configuration. Brittle fracture takes place without preceding plastic deformation, whereas ductile materials can show highly nonlinear behaviour before failure. Correspondingly, different material parameters are used to control the integrity of the structure.

In case of brittle fracture, linear elastic analysis methods are suitable and the stress intensity factor K_I is used to assess the fracture. It governs the stress field near the crack tip as follows (e.g. [1]):

$$\sigma_r = \frac{1}{\sqrt{2\pi r}}\left[K_I\left(\frac{5}{4}\cos\frac{\theta}{2} - \frac{1}{4}\cos\frac{3\theta}{2}\right)\right], \quad (1a)$$

$$\sigma_\theta = \frac{1}{\sqrt{2\pi r}}\left[K_I\left(\frac{3}{4}\cos\frac{\theta}{2} + \frac{1}{4}\cos\frac{3\theta}{2}\right)\right]. \quad (1b)$$

In eqn (1a, b), σ_r and σ_θ are the normal stress components in the polar coordinate system (r, θ) with origin at the crack tip (Fig. 2a).

If the material behaviour is fully ductile, the structural integrity is controlled by the plastic limit load. Between these two extremes, elastic–plastic fracture assessment methods are used and the J-integral by Rice [2] is applied as a fracture parameter

$$J = \int_\Gamma \left(W\,\mathrm{d}y - \mathbf{T}\frac{\partial \mathbf{u}}{\partial x}\,\mathrm{d}s\right), \quad (2)$$

where W is the strain energy density function, $\mathbf{T}$ the traction vector and $\mathbf{u}$ the displacement vector. The

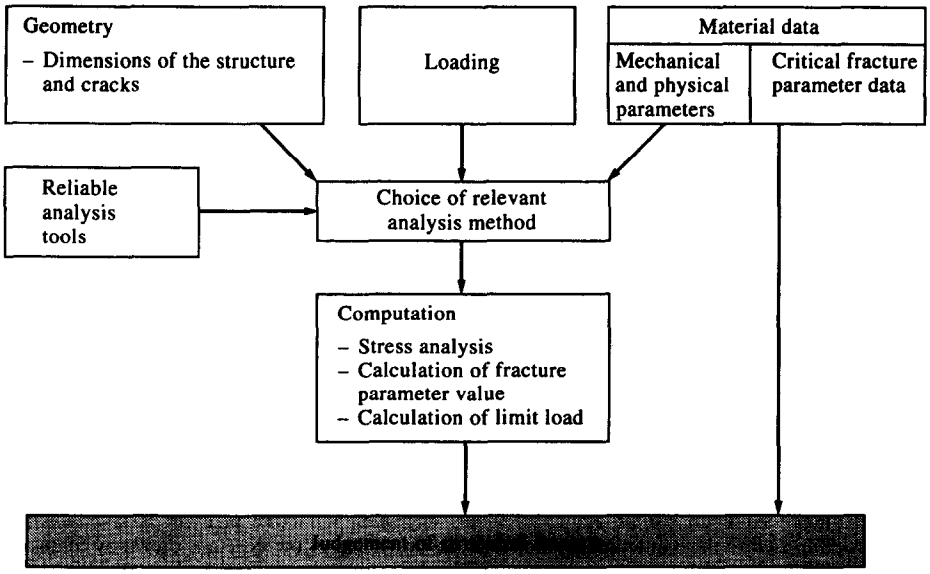

Fig. 1. Principle of solving a structural integrity problem.

J-integral is integrated along the integration path Γ surrounding the crack tip (Fig. 2b).

This paper describes the MASI fracture assessment program system developed at VTT. A few other similar programs exist, such as IWM-BETA [3] and The Fracture Mechanics Toolbox™ [4], which runs under the DOS operating system. The main special feature of the MASI system, however, is that it has primarily been developed for the assessment of nuclear power plant components. Thus, it contains special capabilities for temperature field and stress analysis under pressurised thermal shock loads and for stress intensity factor calculation under steep stress gradients.

2. EVALUATION OF FRACTURE PARAMETER VALUES

The development of methods for computational fracture assessment and experimental fracture toughness definition has made possible the evaluation of highly complex cases. In practice, any case can be solved by applying the finite element method, but even with powerful computers and effective modelling programs this may prove too time-consuming and expensive. Sometimes sudden decisions must be made on component replacement or repair—for example during the annual maintenance outage of a nuclear power plant. In the structural design phase the effect of possible cracks at all critical locations should be checked. For such cases various engineering assessment methods are available.

At VTT several computer programs have been developed for fracture mechanics assessment, especially for nuclear power plant components and structures. There are possibilities for both engineering type assessments and accurate analyses based on the

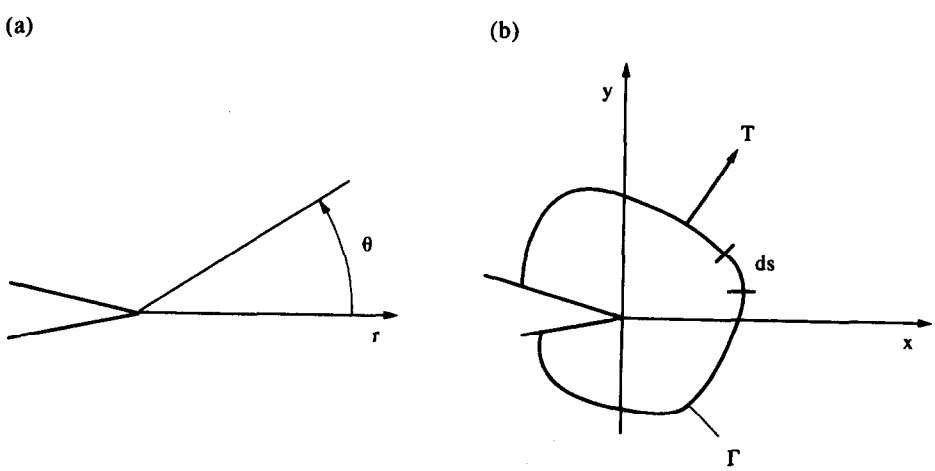

Fig. 2. Crack tip coordinate system (a) and the integration path of the J-integral (b).

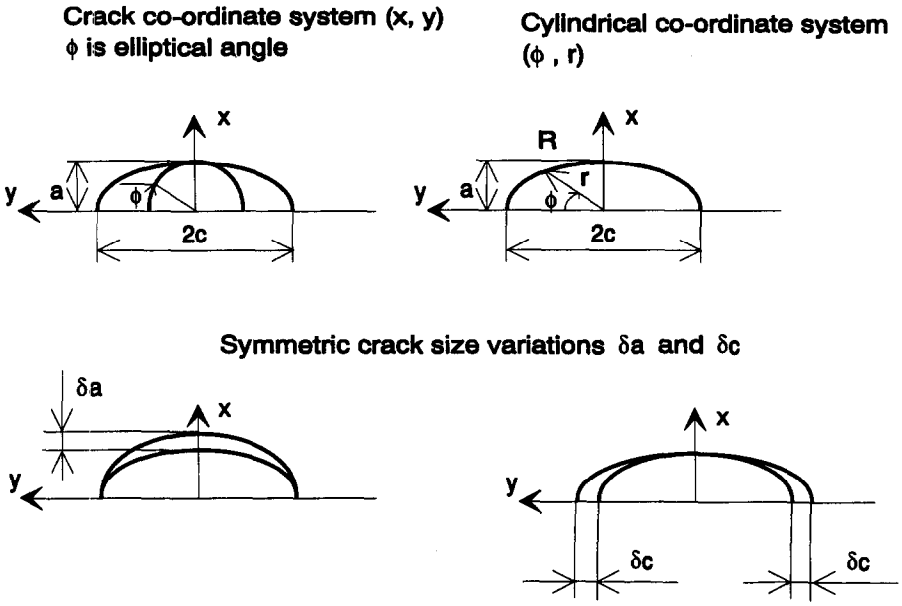

Fig. 3. The semi-elliptical surface crack.

finite element method. The former enable rapid assessments and sensitivity analyses, but may be somewhat rough and unsuitable for special cases. For finite element method applications, programs have been created to simplify accurate analysis of cracked structures.

2.1. *Fracture assessment applying the finite element method*

Using the finite element method (FEM), accurate analyses can be performed for almost any cracked structure. The automatic mesh generation capability provided with the ACR program [5] together with PATRAN greatly simplifies three-dimensional finite element assessments for cracked structures. For stress analysis, general purpose programs ADINA and ABAQUS are mainly used in a workstation which has sufficient computing power for the most practical tasks. The VTTVIRT program [6] has been developed to calculate J-integral values from the stress analysis results obtained with ADINA.

Although many commercial general purpose finite element program packages currently include routines for the evaluation of fracture mechanics parameters, in-house post processing programs are still useful. Elastic–plastic fracture mechanics is still developing and one's own programs provide a possibility to develop and test new parameters.

2.2. *Engineering calculation of stress intensity factor values*

An easy-to-use engineering tool has been developed at VTT for fracture and fatigue analysis. The purpose of the VTTSIF program is to replace the fracture mechanical handbooks for rapid assessments of the stress intensity factor. Crack growth by fatigue is calculated using the Paris equation.

The VTTSIF program applies either direct superposition of reference solutions for different load cases, the weight function method, or a combination of these when calculating the stress intensity factor. It can use either direct weight functions or a weight function approximation method. The applicability of the superposition method is limited by the fact that only a rather small number of stress intensity factor solutions is available and usually only uniform stress is covered for each crack case. Direct weight functions are currently only available for a few basic geometries. The weight function approximation method, on the other hand, requires only an existing stress intensity factor solution typically given as a shape factor by eqn (3):

$$K_{\mathrm{I}} = \sigma_0 Y \sqrt{\pi l} = \sigma_0 F \sqrt{\frac{\pi a}{Q}}, \tag{3}$$

where σ_0 is the scaling stress, Y and F are shape factors, l is crack depth at a location of the crack front, a is crack depth at a location and geometrical parameter characterising the shape of crack front and $\sqrt{Q}$ is the elliptical integral. For elliptical cracks l is

$$l = a\sqrt{\sin^2\Theta + \left(\frac{a}{c}\right)^2 \cos^2\Theta}, \tag{4}$$

where Θ is the elliptical angle and c is the crack length (see Fig. 3). The approximate weight function method can be applied to cases for which the shape factor solution and its derivative with respect to crack size

parameters are available in functional form. Implementation of the weight function method for two-dimensional cases is straightforward and highly accurate results are achieved [7]. For three-dimensional cases, even the evaluation of accuracy is precarious as the accuracy of reference solutions is uncertain. However, experience from practical analyses has shown it to be sufficient in most cases. The theoretical background of the program and some test results have been reported elsewhere [7–10].

The weight function approximation method of the VTTSIF program is based on the Rice formulation [11, 12] in which the stress intensity factor for arbitrary load case denoted by $K_I^{(2)}$ is solved by

$$\int_{\Gamma_c} \frac{K_I^{(1)} K_I^{(2)}}{E'} f_\alpha \, d\Gamma = \int_{A_c} \sigma^{(2)} \frac{\partial \mathbf{u}^{(1)}}{\partial a_\alpha} \, dA \qquad (5)$$

using known stress intensity factor and crack opening displacement solutions for a reference load case denoted by $K_I^{(1)}$ and $\mathbf{u}^{(1)}$ and the stresses at the crack plane in an uncracked structure under the arbitrary load case denoted by $\sigma^{(2)}$. In eqn (5), E' is the effective Young's modulus and the left side is integrated along the crack front Γ_c and the right side over the crack plane A_c (Fig. 3). The Rice formulation of the weight function method is given for arbitrary crack size variation δa_α which is mapped along the crack front by function f_α. For two-dimensional cases this reduces to crack depth variation $\delta a_1 = \delta a$ and to $f_1 = 1$. For three-dimensional cases solutions are available only for elliptical crack shapes, and the variations must sustain the elliptical crack shape. Consequently, the possible variations reduce to a maximum of three for semi-elliptical surface cracks and a maximum of four for embedded elliptical cracks. Symmetry in loading would further reduce the variations to a minimum of two, as shown in Fig. 3.

At present the solutions available in the VTTSIF program are limited to crack opening mode *I*. They cover 10 two-dimensional geometry cases for which 19 different solutions originating from the literature are available. The two-dimensional solutions include several basic solutions, such as an edge crack in a finite width strip, as well as crack cases in cylindrical geometry (Table 1). The six three-dimensional geometry cases cover an embedded elliptical crack in an infinite solid, semi-elliptical surface crack in a plate and in a cylinder. The crack cases in cylinder geometry include inner and outer surface axial cracks and inner surface circumferential cracks. Another real geometry case is a semi-elliptical surface crack on the inner surface of a pressure vessel nozzle connecting weld. A total of 15 different load case solutions are available for these crack cases, comprising a uniform stress solution for all and bending or linear stress solution for most cases. Two different solutions are available for the semi-elliptical surface crack in a plate. They have been presented by Newman and Raju [13] and by Mikkola [7]. Both cases are available for tension and bending load.

New solutions have also been developed for a surface crack in a weld connecting a nozzle to a pressure vessel [9] and for axial semi-elliptical surface cracks on the inner and outer surfaces of a cylinder [10]. They were developed by curve-fitting finite element results to rational polynomials. The finite element results were calculated by the ADINA and VTTVIRT programs and the finite element

Table 1. Structure/crack configurations in the VTTSIF program

Structure	Crack type	Crack case
Semi-infinite solid	Two-dimensional, through thickness	Edge crack
Infinite solid	Three-dimensional, elliptical	Embedded crack
Finite width strip	Two-dimensional, through-thickness	Edge crack Centre crack Double edge crack
Plate	Three-dimensional, semi-elliptical	Surface crack
Disk	Two-dimensional, through-thickness	Radial crack
Shaft	Two-dimensional, circumferential 360°	Radial crack
Cylinder	Two-dimensional, circumferential 360°	Radial inner surface crack Radial outer surface crack
	Two-dimensional, infinitely long	Axial inner surface crack Axial outer surface crack
	Three-dimensional, semi-elliptical	Circumferential inner surface crack Axial inner surface crack Axial outer surface crack
Cylinder nozzle	Three-dimensional, semi-elliptical	Surface crack in a RPV/nozzle weld

Table 2. Structure/crack configurations in the LIMIT program

Structure	Crack case	Loading case
Plate	Through-thickness crack	Tension + bending
	Long surface crack	Tension + bending
	Semi-elliptical surface crack	Tension + bending
	Elliptical embedded crack	Tension + bending
Spherical shell	Through-thickness crack	Internal pressure
	Semi-elliptical surface crack	Internal pressure
Round bar	Axisymmetric sharp notch	Tension
		Torsion
	Chordal crack	Bending
		Torsion
Cylinder, axial crack cases	Long inner surface crack	Internal pressure
	Long outer surface crack	Internal pressure
	Semi-elliptical inner surface crack	Internal pressure
	Semi-elliptical outer surface crack	Internal pressure
	Through-wall crack	Internal pressure
Cylinder, circumferential crack cases	Complete (360°) inner surface crack	Tension + bending
	Semi-elliptical inner surface crack	Tension + bending
		Internal pressure
	Through-wall crack	Tension + bending
Pipe bend	Defect-free	Internal pressure
		Bending
	Longitudinal through-wall defect	Internal pressure
		Bending
	Circumferential through-wall defect	Internal pressure
		Bending
Cylinder–cylinder intersection	Inner and outer corner cracks	Internal pressure

models were automatically generated by the ACR program. In the case of the plate geometry [7] the finite element data covered the same crack size matrix as used by Newman and Raju [13] and other data for several limiting solutions taken from the literature. The developed solution was used for verification of the system and demonstrated the possibility of generating new three-dimensional solutions.

2.3. *Evaluation of the plastic yield load of a cracked structure*

Plasticity effects are included in the R6 failure assessment procedure [14, 15] by means of parameter L_r which is a measure of how close to plastic yielding the structure containing the crack is. L_r is defined as the ratio of the loading condition being assessed to that required to cause plastic yielding of the structure. The plastic yield load depends on the strength of the material and also on the geometry of the crack to be assessed. Functions are given in the literature [16, 17] for analytical or approximate solutions of parameter L_r. A set of these functions is coded in a computer program, LIMIT [18]. The LIMIT program is an in-house product of VTT.

The yield load usage factors L_r included in the LIMIT program contain basic crack cases in flat plates, cylindrical and spherical shells, round bars, pipe bends and cylinder-to-cylinder intersections. They are summarized in Table 2.

2.4. *Thermal and stress analysis of a pressurized thermal shock in a cladded pressure vessel*

The thermal transient analysis in axisymmetric geometry is performed very quickly by the DIFF program [19], which is also an in-house product of VTT. The program is highly efficient and can easily be used in normal PC hardware with reasonable running times.

DIFF can handle temperature dependent material properties, two-layer cladded walls, time dependent boundary conditions, inside and outside temperature and heat transfer coefficients on the surface. The thermal transient analysis is based on solution of the heat transfer equation in axisymmetric geometry by the method of finite differences. The program can handle simultaneously two sets of thermal boundary conditions in axisymmetric geometry, allowing an approximation of the effects of circumferentially varying cooling zones. This is the case if the coolant flow is quite low and/or the coolant temperature is very low compared with mixed conditions inside the vessel. The program performs a check on time step length proposed by the user and gives a better estimate in case the stability check is negative. During

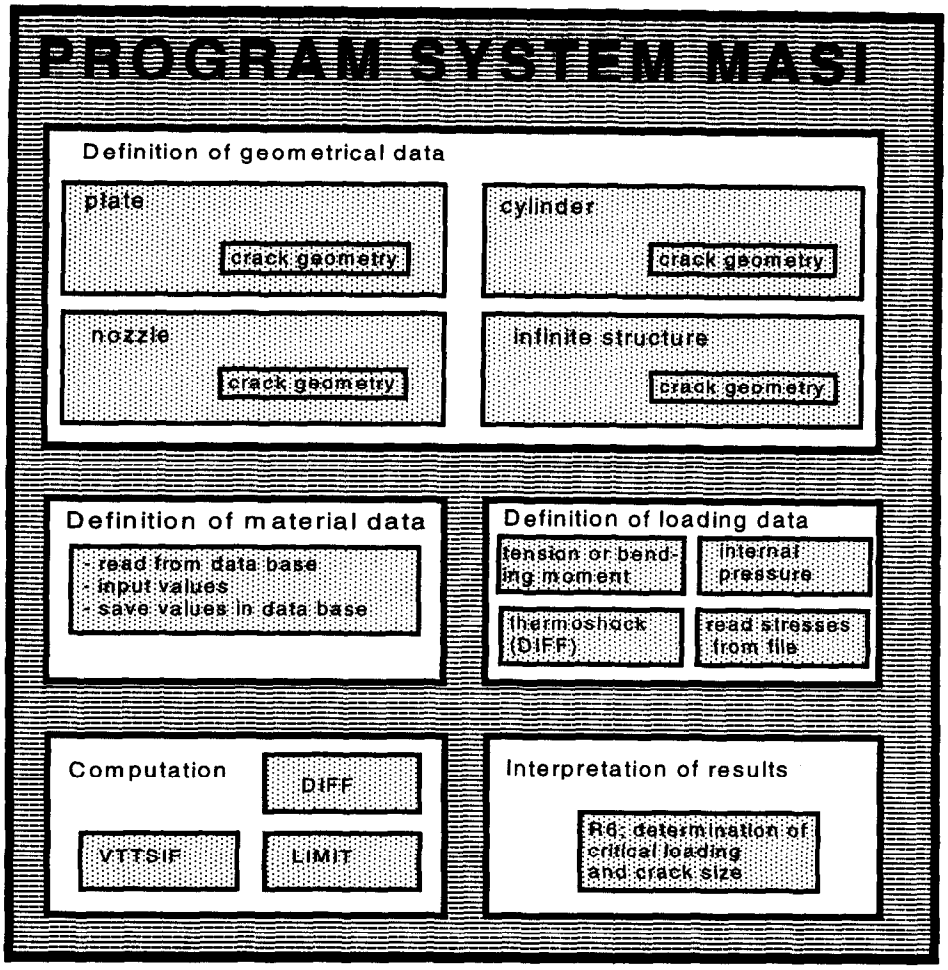

Fig. 4. General structure of the MASI program system.

analysis, the program monitors the stability of the solution and gives warning of suspected instability.

Besides thermal analysis, the program calculates the stress state of the cylinder due to thermal and pressure loads. The stresses are calculated according to the analytical solution of stresses for a thick cylindrical shell, based on liner material behaviour according to Hooke's law. The program handles the stress-free temperature of the bimetallic structure as an input parameter.

3. THE INTEGRATED MASI PROGRAM SYSTEM

One drawback in applying fracture mechanics to practical problems is that often the computer programs can only be used by specialists or developers. To use the computing tools reliably requires good knowledge of fracture mechanics and experience of the particular program. Besides, the programs are often run on computers with unnecessarily large computing power for the problem at hand. Fairly computing intensive tasks can today be performed on a PC. The compatibility of FORTRAN compilers for PCs, like Microsoft FORTRAN 5.1, with FORTRAN compilers in mainframe computers has been increased, and built-in mathematical coprocessors simplify transformation or the "right-sizing" of programs. In the Windows environment large problems can be run effectively, whereas the DOS system is hampered by severe CPU memory restrictions.

3.1. *The components of the MASI system*

If several independent programs are needed to analyse a practical case, problems often arise in data exchange and compatibility between them. By

Table 3. Physical and mechanical material properties applied in the spinning cylinder example

	Cladding material	Base material
Thermal conductivity ($N\,s^{-1}\,K^{-1}$)	15.3	33.92
Thermal expansion coefficient ($1°C^{-1}$)	$18.5*10^{-6}$	$13.4*10^{-6}$
Specific heat per unit volume ($N\,m^{-2}\,K^{-1}$)	$3.92*10^{6}$	$4.21*10^{6}$
Young's modulus (GPa)	179	189

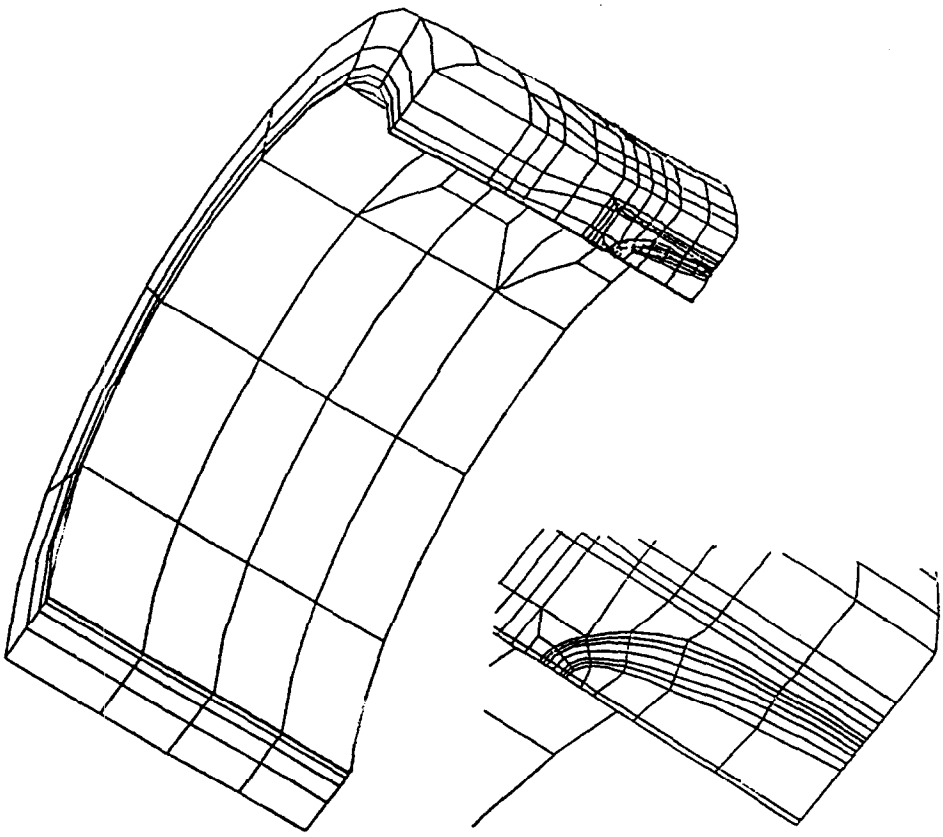

Fig. 5. The finite element model used in the calculation of the spinning cylinder example [22].

integrating different engineering assessment programs and improving their user friendliness, one can use them effectively together to solve complex problems. For this purpose the integrated program system MASI has been developed [20]. The programs based on engineering assessment methods have been implemented in a PC computer and a graphic user interface has been developed for them.

The general layout of the MASI is shown in Fig. 4. The system combines three basic components: the user interface, the computational part and the material data base. In cases where engineering methods cannot yield a solution with sufficient

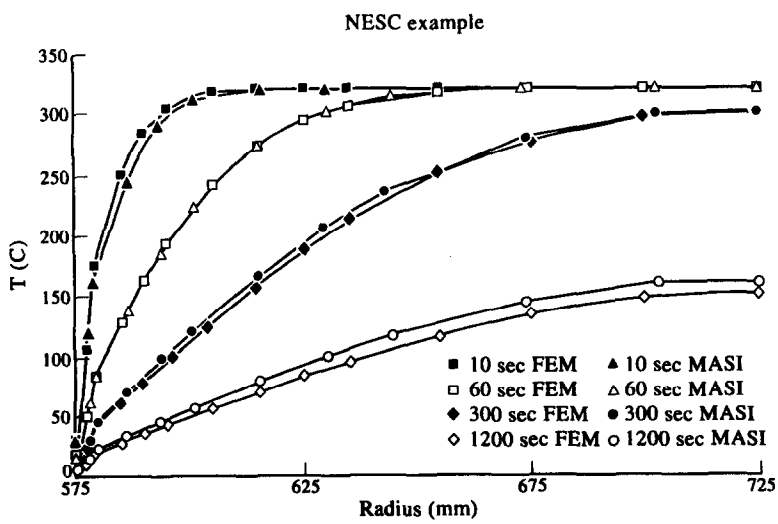

Fig. 6. Temperature distribution along the radius as a function of time for the spinning cylinder example. Comparison of MASI results with FEM results of Ref. [22].

accuracy, the user is advised to apply the finite element method.

The MASI program system is aimed primarily at helping a structural analyst judge the severity of detected or postulated cracks and the allowable crack size. The computational part of the program system comprises the FORTRAN programs DIFF, VTTSIF and LIMIT, which were originally developed in mainframe or workstation computers and then converted to Microsoft FORTRAN. These programs are implemented into the MASI system as executable files and they are run and coordinated by the user interface.

3.2. *The user interface*

The event-driven graphical user interface has been developed using Visual Basic, as this is a very easy-to-use tool for creating Windows applications. It handles the following tasks:

(1) to help the user model the problem by simplifying the input of crack/structure configuration and the treatment of loads;
(2) to exchange data between different programs;
(3) to control execution of the computing programs;
(4) to judge the structural integrity;
(5) to report and visualize the results.

In the modelling phase, the crack/structure configuration must be simplified so that the problem can be solved by applying the available stress intensity factor and limit load solutions. When the weight function method is used, stress intensity factor values can be calculated for any stress distribution. In three-dimensional crack cases, however, even this approach may be too time-consuming, especially if many crack sizes and load steps are calculated. One example is the assessment of crack initiation and arrest in a reactor pressure vessel under pressurized thermal shock (PTS) loading. The stress intensity factor calculation is much faster if loading can be treated with superposition of available stress intensity factor solutions instead of applying the weight function method directly.

For instance a PTS problem is solved using MASI according to the following four steps:

(1) Input the geometric, material as well as thermal loading parameters in the geometry, material and loading modules of MASI.
(2) Generate a DIFF input file and start the DIFF program in the computing module of MASI and perform the thermal shock loading.
(3) Generate VTTSIF input files by internally reading the output results of DIFF. Run VTTSIF and obtain the stress intensity factors for fracture assessment.
(4) Present the results as a stress intensity factor vs crack tip temperature diagram.

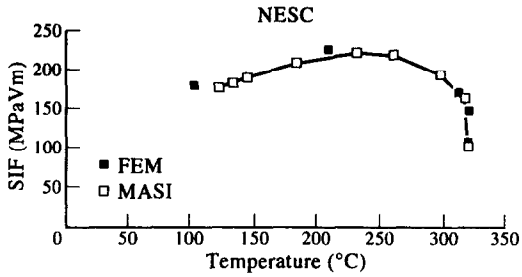

Fig. 7. Stress intensity factors (SIF) as a function of crack tip temperature for the spinning cylinder example. Comparison of MASI results with FEM results of Ref. [22].

For judging structural integrity between the two extremes of brittle fracture and plastic limit load, at present the R6 method revision 2 option 1 [15] can also be applied. If the point corresponding to the particular case lies inside the failure curve, the structural integrity is retained. Further conclusions can be drawn on safety factors for loading and allowable crack size.

4. COMPUTATIONAL EXAMPLES

4.1. *The spinning cylinder example*

As the first cooperative task of the European Network for Evaluation of Steel Components, NESC, experimental and computational studies for thermal shock experiment with a cladded spinning cylinder specimen are being conducted by several organizations [21]. The actual test will be performed at AEA Technology in the United Kingdom. Experimental studies will comprise extensive material characterization, nondestructive testing, and on-line measurement programmes. Detailed three-dimensional finite element models and different engineering analysis methods will be applied in the computational analyses.

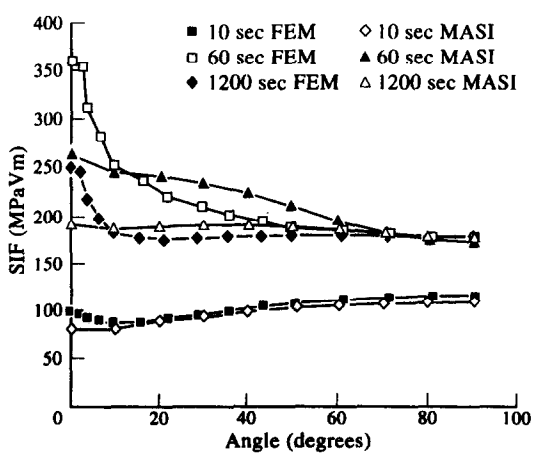

Fig. 8. Stress intensity factor distribution along the crack front as a function of time for the spinning cylinder example. Comparison of MASI results with FEM results of Ref. [22].

Table 4. Physical and mechanical material properties applied in the VVER-440 reactor pressure vessel example [23]

		Cladding material	Base material
Thermal conductivity ($N\,s^{-1}\,K^{-1}$)	20°C	15.1	40.2
	300°C	18.8	37.9
Thermal expansion coefficient ($1°C^{-1}$)	20°C	$16.3*10^{-6}$	$11.3*10^{-6}$
	300°C	$17.4*10^{-6}$	$13.1*10^{-6}$
Specific heat per unit volume ($N\,m^{-2}\,K^{-1}$)	20°C	$3.6*10^{6}$	$3.92*10^{6}$
	300°C	$4.18*10^{6}$	
Young's modulus (GPa)	20°C	205	210
	300°C	180	195

The inner radius of the open cylinder is 575 mm, the cladding thickness 4 mm and the cylinder thickness including the cladding 150 mm. For the present verification purposes, an axial semi-elliptical through-cladding crack with a depth of 64 mm and a half crack length of 180 mm was considered. The material parameter values shown in Table 3 were used in the calculations.

In pre-test analyses, the DIFF and VTTSIF programs of MASI were utilized. The hoop stress distribution arising from the rotation was calculated from the formula.

$$\sigma_\Theta = \frac{\rho\omega^2}{8} * \frac{3-2\nu}{1-\nu} * \left[R_1^2 + R_2^2 + \frac{R_1^2 R_2^2}{R^2} - 3R^2 \right] + \rho\omega^2 R^2 \quad (6)$$

and superposed on the DIFF results. In eqn (6) ω is the rotational speed, ρ is the density of the material, ν is Poisson's ratio, R is the location, and R_1 and R_2 are the inner and outer radii of the cylinder.

Starting from the initial temperature of 320°C, axisymmetric cooling with 5°C cooling water was applied to the inner surface. The heat transfer coefficient values at the inner and outer surfaces were 22,000 $W\,m^{-2}\,K^{-1}$ and 8 $W\,m^{-2}\,K^{-1}$, respectively, and the stress free temperature was taken as 320°C. The rotational speed of the cylinder was 2500 rpm.

This case was also calculated by applying the finite element model shown in Fig. 5 [22]. In Figs 6–8 the MASI results are compared with the results of the thermoelastic finite element analysis. Figure 6 shows the calculated temperature distribution through the wall thickness as a function of time. In Fig. 7, the stress intensity factor values (SIF) are presented as a function of crack tip temperature. Both figures show good agreement between the MASI and finite element results. The stress intensity factor distribution along the crack front as a function of time is shown in Fig. 8. Near the free surface the stress intensity factor values calculated by MASI are clearly lower than those obtained using the finite element method. Due to the assumed semi-elliptical crack variation (Fig. 3), the weight function method does not yield an accurate value at that location.

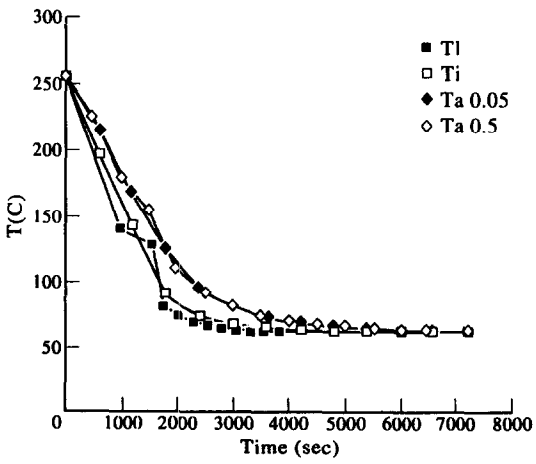

Fig. 9. Coolant temperature Tl and calculated pressure vessel wall temperatures at inner surface (T_i) and at crack tip position (T_a) in the strip area as a function of cooling time for the VVER-440 pressure vessel example. T_a values are presented corresponding to two different time step values (0.5 and 0.05 s).

4.2. *Pressurized thermal shock analysis for a VVER-440 reactor pressure vessel*

A cladded VVER-440 reactor pressure vessel with a hypothetical circumferential surface crack in a core region weld was re-analysed by MASI. The loading

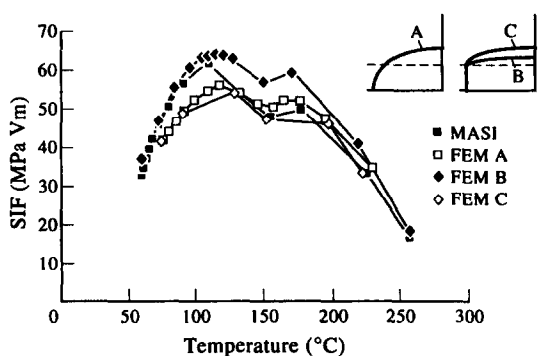

Fig. 10. Fracture assessment results: stress intensity factor as a function of crack tip temperature at the deepest point of the crack for the VVER-440 pressure vessel example.

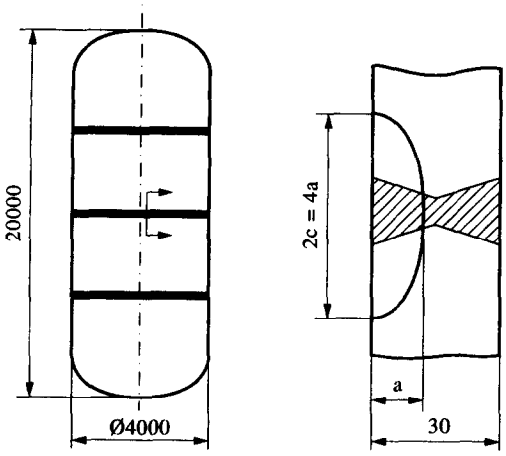

Fig. 11. The geometry of the pressure vessel in the R6 application example [16].

was a thermal-mechanical transient due to loss of coolant with high pressure injection. Extensive three-dimensional thermoplastic finite element analyses were performed by GRS Germany, IVO International Ltd. and VTT [23].

The inner radius of the cylinder was 1771 mm, the cladding thickness 9 mm and the cylinder thickness including the cladding 149 mm. Nonaxisymmetric cooling through one nozzle only was assumed and the width of the cooling area in the circumferential direction was taken as 540 mm. A semi-elliptical crack with a depth of 15 mm and a half crack length of 25 mm was considered and the material parameter data of Table 4 was used. In one of the FE models the crack depth was 12 mm only.

The loading was defined by a constant internal pressure of 13.7 MPa and by time-dependent coolant temperatures in the strip area (the temperature at the height of the nozzle, T_1) and in the mixed area (T_{mix}). In reality there was an axial variation in the coolant temperatures within the strip so that the coolant temperature at the crack level was slightly higher than at the nozzle location. Thus it is a somewhat conservative approach to apply the nozzle temperatures as the loading for the whole strip length. The heat transfer coefficient value at the mixed area was taken as 2000 W m^{-2} K^{-1}. In the strip area it was set to 2000 W m^{-2} K^{-1} until 1550 s from the start of cooling and 5000 W m^{-2} K^{-1} subsequently. At the outer surface the heat transfer coefficient was taken as 8 W m^{-2} K^{-1}.

Table 5. The R6 application example: comparison of L_r values obtained using MASI with the results of the INSTA report [16]

a (mm)	L_r MASI	L_r Ref. [16]
1	0.86	0.87
2	0.87	0.87
3	0.88	
4	0.89	0.89
5	0.90	
6	0.92	0.93
7	0.94	
8	0.96	0.98

The temperature and stress distributions were calculated using the DIFF program and the stress results were used in the stress intensity factor calculation with VTTSIF. Figure 9 compares the coolant temperature $T1$ and the calculated temperatures as a function of cooling time. Two time increment sizes were used. The figure shows that the increment size has no great influence on the results. Stress intensity factor as a function of crack tip temperature at the deepest point of the crack is compared in Fig. 10 with the finite element results obtained elsewhere [23]. The differences among the finite element results can be explained by differences in modelling, like crack depth and shape (Fig. 10), description of the asymmetry of the cooling strip, and consideration of welding residual stresses. Only in FEM analysis C was the cooling strip asymmetry considered. In FEM analysis B and in the MASI calculation a conservative approach was used to treat the welding residual stresses: a stress intensity factor value of 3.5 MPa$\sqrt{m}$ corresponding to a constant tensile stress of 60 MPa at the crack location in the weld was superposed on the calculated values. Taking the small computing effort into account, the MASI results can be said to correlate very well in this case with the finite element results.

4.3. *Re-assessment of cracks in a pressure vessel by MASI*

The original assessment of this example is documented in the INSTA Technical Report [16]. An internal axial crack was located symmetrically across the circumferential weld of a cylindrical pressure vessel (Fig. 11). The outer diameter of the cylinder was 4000 mm and the wall thickness 30 mm. The design yield stress at the operation temperature of 220°C was $\sigma_y = 170$ MPa and the corresponding critical stress intensity factor value $K_{Ic} = 77$ MPa$\sqrt{m}$ [16]. According to a constant internal pressure of 2.2 MPa, the hoop stress was $\sigma_h = 145.6$ MPa. It was used as the primary stress σ_p, and the welding residual stress of 300 MPa as the secondary stress σ_s.

Semi-elliptical edge cracks with a fixed $a/c = 0.5$ were considered. The crack depth varied from 1 to 8 mm. LIMIT and VTTSIF programs were applied. A limit load solution for a cracked cylinder was adopted, but due to the small curvature of the shell a stress intensity factor solution for a semi-elliptical surface crack in a plate was used. In Tables 5 and 6 the L_r and K_r values calculated using MASI are compared with the results of the INSTA report [16]. The presented K_r values have been calculated at the deepest point of the crack. In both cases a good agreement is obtained. Figure 12 shows the R6

Table 6. The R6 application example: comparison of K_r values obtained using MASI with the results of the INSTA report [16]

a (mm)	$K = K_I^p + K_I^s$ (MPa$\sqrt{m}$) [16]	$K = K_I^p + K_I^s$ (MPa$\sqrt{m}$) MASI	$K_r = K/K_{Ic}$ MASI	$K_\rho = K_I^p + K_I^s + \rho(a)$ (MPa$\sqrt{m}$) MASI	$K_{r\rho} = K_\rho/K_{Ic}$ MASI
1	22.6	22.4	0.291	29.98	0.389
2	32.1	31.7	0.412	39.08	0.508
3		39.0	0.507	46.00	0.597
4	45.8	45.3	0.588	51.80	0.673
5		51.0	0.662	56.93	0.739
6	56.5	56.3	0.731	61.57	0.800
7		61.3	0.796	65.89	0.856
8	67.1	66.2	0.860	69.96	0.909

assessment results with and without ρ-correction, which covers the interactions between primary and secondary stress categories [16]. From Fig. 12 it can be concluded that the critical crack depth corresponding to the initiation of crack growth at the operation temperature is about 4.5 mm, while a more accurate study in the INSTA report [16] yielded the value of 4.38 mm.

5. SUMMARY

This paper outlined an easy-to-use program system (MASI) for fracture assessment. The program system is intended as a user-friendly computing tool, which runs in a microcomputer under the Windows environment. It comprises the independent FORTRAN programs DIFF for calculation of temperature and stress distributions in a pressurized thermal shock loading, VTTSIF for computing stress intensity factor values and LIMIT for plastic limit load calculation. The programs are controlled and executed by a graphical user interface developed using Visual Basic.

The purpose of the MASI system is to replace fracture mechanical handbooks for rapid assessments of the integrity of cracked structures. It can be used, for example, for studying the criticality of several load cases combined with cracks in various locations of the structure. It supports more accurate studies by the finite element method, as it can use the stress results from finite element analysis for uncracked structures.

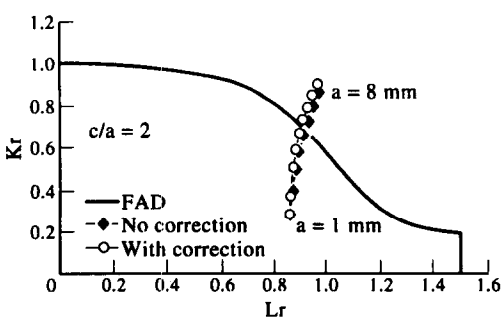

Fig. 12. R6 assessment results, with and without ρ-correction for the pressure vessel example.

The applicability and accuracy of the system has been proven within several domestic and international research programmes. Using three computational examples it was shown that the highly effective engineering assessment tools may yield results which agree very well with those obtained using extensive elastic–plastic three-dimensional finite element analyses. However, in case of a cladded pressure vessel wall the agreement is good only at the deepest point of the crack. The different properties of base and cladding materials cause a steep stress gradient at the cladding/base material interface. In such cases the VTTSIF program can yield only approximate stress intensity factor values in the cladding and cladding/base material interface areas.

Acknowledgements—This work is a part of the project "Technical Service Life Determination of Reactor Pressure Vessels and Piping (PAPU)" in the research programme "Nuclear Power Plant Structural Safety (RATU)" and has been funded by the Ministry of Trade and Industry and the Technical Research Centre of Finland.

REFERENCES

1. D. Broek, *Elementary Engineering Fracture Mechanics*. Martinus-Nijhoff, The Hague, The Netherlands (1984).
2. J. R. Rice, Some remarks on elastic crack-tip stress fields. *Int. J. Solids Struct.* **8**, 751–758 (1972).
3. L. Hodulak and C. Butterweck, Rechenprogramm IWM-BETA Version 1.4. Fraunhofer-Institut für Werkstoffmechanik, Freiburg (1989).
4. Anonymous, *Introducing the Fracture Mechanics Toolbox*™. Reflex Engineering, Pacific Grove (1993).
5. M. Leinonen and T. P. J. Mikkola, The ACR-program for automatic finite element model generation for part through cracks. Research Reports 658, Technical Research Centre of Finland (VTT), Espoo (1989).
6. H. Talja, Calculation of elastic–plastic fracture parameters using the finite element method. Licentiate Thesis, Helsinki University of Technology, Espoo (1987) (in Finnish).
7. T. P. J. Mikkola, Method for calculating stress intensity factors for surface cracks. *Engng Fract. Mech.* **42**, 713–730 (1992).
8. T. P. J. Mikkola, *Numerical Analysis Methods of Surface Cracks*. Technical Research Centre of Finland, Espoo, VTT Publications 119 (1992).
9. T. P. J. Mikkola, Applications of the weight function method. *Engng Fract. Mech.* **45**, 209–231 (1993).
10. T. P. J. Mikkola, Development of VTTSIF reference cases for axial surface cracks on inner and outer surface

of a cylinder. Technical Report LAI93107, Technical Research Centre of Finland, Ship Laboratory, Espoo, (1993).

11. J. R. Rice, A path independent integral and the approximate analysis of strain concentration by notches and cracks. *J. appl. Mech. Trans. ASME* **35,** 751–758 (1968).
12. J. R. Rice, Weight function theory for three-dimensional elastic crack analysis. In: *Fracture Mechanics: Perspectives and Directions (Twentieth Symposium)* (Edited by R. P. Wei and R. P. Gangloff), ASTM STP 1020, pp. 29–57. American Society for Testing and Materials, Philadelphia (1989).
13. J. C. Newman and I. S. Raju, Stress-intensity factor equations for cracks in three-dimensional finite bodies. In: *Proc. Fracture Mechanics: Fourteenth Symp.*, Vol. I: *Theory and Analysis* (Edited by J. C. Lewis and G. Sines), pp. 238–265. American Society for Testing and Materials (1983).
14. R. P. Harrison, L. Loosemore and I. Milne, Assessment of the integrity of structures containing defects. CEBG Report R/H/R6 (1976).
15. I. Milne, R. A. Ainsworth, A. R. Dowling and A. T. Stewart, Assessment of the Integrity of Structures Containing Defects. *Int. J. Press. Vessels Piping* **32,** 3–104 (1988).
16. Anonymous, Assessment of the integrity of structures containing discontinuities. INSTA Technical Report, Materials Standards Institution, Stockholm (1991).
17. A. G. Miller, Review of limit loads of structures containing defects. *Int. J. Press. Vessels Piping* **32,** 197–327 (1988).
18. H. Raiko, The plastic limit load of cracked structures. Work report LUJA-2/93, Technical Research Centre of Finland (VTT), Espoo, (1993) (in Finnish).
19. H. Raiko, K. Ikonen and T. P. J. Mikkola, DIFF, an analysis program for PTS. Work report LUJA-1/94, Technical Research Centre of Finland (VTT), Espoo (1994) (in Finnish).
20. H. Talja, Program System MASI for Fracture Assessment. Version 1.0 Status report and user instructions. Report VALB43, Technical Research Centre of Finland (1995).
21. Anonymous, Networking for improved structural integrity assessment. *Nucl. Engng Int.* **38,** 21–24 (1993).
22. H. Talja, Preliminary computational analyses for the NESCI project. Report VALB42, Technical Research Centre of Finland, Espoo (1994).
23. J. Sievers, X. Liu, P. Rajamäki, H. Talja and H. Raiko, Comparative analyses concerning integrity of a VVER-440 reactor pressure vessel. *Nucl. Engng Des.* **159,** 63–68 (1995).